


Different Critical Exponents on Two Sides of a Transition: Observation of Crossover from Ising to Heisenberg Exchange in Skyrmion Host Cu_2OSeO_3

Harish Chandr Chauhan, Birendra Kumar, Ankita Tiwari, Jeetendra Kumar Tiwari, and Subhasis Ghosh^{*}
School of Physical Sciences, Jawaharlal Nehru University, New Delhi 110067, India

 (Received 29 June 2021; revised 25 September 2021; accepted 9 December 2021; published 4 January 2022)

We present experimental investigation on critical phenomena in Cu_2OSeO_3 by analyzing the critical behavior of magnetization using a new method. This is necessary as a crossover from 3D Ising to 3D Heisenberg has been observed in Cu_2OSeO_3 . The proposed method is applicable to explore the physics for a wide range of materials showing trivial or nontrivial critical behavior on two sides of the transition. A magnetic phase diagram has been constructed from the critical analysis. Multiple critical points due to multiple phases and transition between them have been observed in the phase diagram of Cu_2OSeO_3 .

DOI: [10.1103/PhysRevLett.128.015703](https://doi.org/10.1103/PhysRevLett.128.015703)

Skyrmions have been observed in several materials with different crystal symmetries [1–7]. In noncentrosymmetric systems [1–5,7], skyrmionic phase emerges due to the competition between symmetric exchange interaction (SEI) and antisymmetric Dzyaloshinskii-Moriya interaction (DMI) [8,9]. The role of DMI has been established beyond a doubt for the formation of skyrmion, but the nature of SEI remains an open question: Is it Heisenberg type or Ising type? Based on renormalization group (RG) theory, various models have been developed to explain the critical behavior of magnetic systems to reveal the exact nature of spin-spin interaction. The critical behavior of a system is defined by a set of critical exponents [10] for different universality classes (UCs) depending on the nature of spin-spin interactions, such as Heisenberg, Ising, or XY for which β and γ are 0.365 and 1.386, 0.325 and 1.241, and 0.345 and 1.316, respectively [10], where β is the critical exponent associated with magnetization and γ is the critical exponents associated with susceptibility. Rarely, mean-field values of β ($= 0.5$) and γ ($= 1.0$) are observed in real systems. Moreover, RG theory posits that the critical behavior should be similar below and above the transition temperature T_C , which is defined as the temperature above which order parameter becomes zero. Here, we pose an important question: Is it possible to have different critical behavior below and above T_C ? Nelson [11] first addressed this nontrivial problem. Here, trivial systems are those which follow RG theory. Subsequently, Léonard and Delamotte [12] showed theoretically that there is the possibility of different critical behavior below and above T_C . Recently obtained critical exponents for some systems, such as FeGe [13] ($\beta = 0.336 \pm 0.004$ and $\gamma = 1.352 \pm 0.003$) and $\text{Pr}_{0.6-x}\text{Er}_x\text{Ca}_{0.1}\text{Sr}_{0.3}\text{MnO}_3$ [14] ($\beta = 0.355 \pm 0.008$ and $\gamma = 1.294 \pm 0.012$ for $x = 0.06$) do not belong to a single UC. For FeGe, β is close to three-dimensional (3D) Ising UC and γ is close to 3D Heisenberg UC. For

$\text{Pr}_{0.6-x}\text{Er}_x\text{Ca}_{0.1}\text{Sr}_{0.3}\text{MnO}_3$, β is close to 3D Heisenberg UC while γ is close to 3D Ising UC. Thus, the conclusions obtained from such critical exponents may be ambiguous. These results indicate that the critical behavior of nontrivial systems may be different on two sides of the transition. This brings back another important question: How can one investigate the critical behavior of nontrivial systems? To investigate the critical phenomena in nontrivial systems, we present a new method, i.e., the modified iteration method (MIM), to investigate the critical behavior of skyrmion host Cu_2OSeO_3 —a nontrivial system.

Cu_2OSeO_3 is skyrmion host insulating chiral cubic B20 material with space group $P2_13$. The competition between SEI and DMI results in the formation of multiple phases, such as multidomain helical (MDH), single domain conical (SDC), skyrmion [5,15], and fluctuation disordered (FD) phase [16,17]. All these phases lead to rich phase diagram due to multiple phase transitions with two phase boundaries defined by (i) first-order phase transition (FOPT) from helimagnetic to FD phase with transition temperature at T'_C [16,17] and (ii) second-order phase transition (SOPT) from FD to paramagnetic phase with transition temperature at T_C [7,16]. The FOPT at T'_C and SOPT at T_C have been established by magnetization [16], entropy [16], and specific heat [17] measurements. Similar phase diagrams with two transition temperatures have been observed in other skyrmion host materials such as MnSi [1,7], FeGe [2], and $\text{Fe}_{0.8}\text{Co}_{0.2}\text{Si}$ [3]. After FOPT at T'_C , as shown in Fig. 1, DMI decreases faster with temperature relative to SEI. Between T'_C and T_C , SEI and DMI result FD phase [18] which has been experimentally confirmed by small angle neutron scattering [19]. Moreover, Cu_2OSeO_3 has two types of CuO_5 polyhedra—square pyramidal and trigonal bipyramidal in the ratio of 3:1—which leads to the formation of two sublattices [20]. This causes the emergence of the magnetocrystalline anisotropy in the system

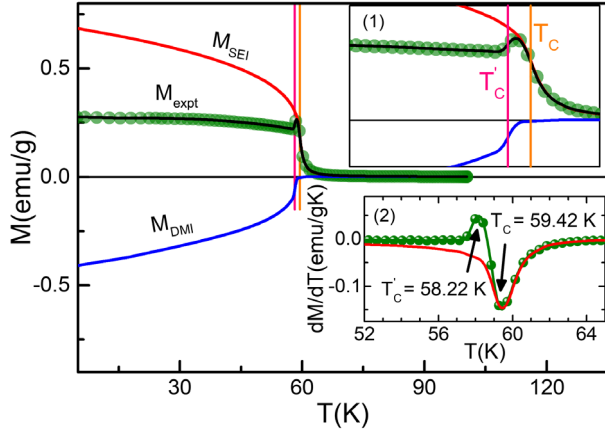


FIG. 1. Temperature-dependent magnetization (M - T) of Cu_2OSeO_3 measured without applying field. The red solid line represents the expected variation of the moment due to SEI (M_{SEI}) and the blue solid line represents the variation of magnetic moment due to DMI (M_{DMI}). Black solid line is the spline fit to the experimental data. Inset (1) is the expanded view of the M - T in the vicinity of T_C . Inset (2) shows the first derivative (dM/dT) of the M - T . The minimum of the dM/dT gives $T_C = 59.42$ K, and maximum of the dM/dT represents $T'_C = 58.22$ K. Solid red line represents the derivative of the M - T corresponding to M_{SEI} .

with easy axis along [111] [19,24]. Thus, below T_C , the phase transition and the critical phenomena will be facilitated by SEI, DMI, and anisotropy. Generally, DMI is weaker than Ising or Heisenberg exchange interaction [9,25]. DMI is substantially reduced above T'_C and practically becomes ineffective above T_C [26,27]. Hence, the interactions responsible for the evolution of different phases below and above T_C are different. This means the interactions in Cu_2OSeO_3 lead to a situation where Wilson-Fisher theory of critical phenomena [28,29] becomes nontrivial.

In this Letter, we present our experimental investigation on phase transition and critical phenomena in Cu_2OSeO_3 to address mainly two issues: (i) the type of the SEI responsible for different phases below T_C and (ii) crossover from one critical behavior to another critical behavior below and above T_C . We show that the critical exponents obtained by iteration method and change in entropy do not match well with the critical exponents for a single standard UC for the reasons discussed previously. To investigate the different critical behaviors and to obtain the critical exponents below and above T_C , a new method of critical analysis has been developed. While addressing these issues, we have shown that it is possible to construct the phase diagram, which generally agrees with the generic phase diagram of skyrmion host B20 materials. Multiple critical points, such as tricritical point, Lifshitz point, and triple point, have been observed from the constructed phase diagram.

Magnetization measurements were carried out using physical properties measurement system [20]. In the

vicinity of T_C , temperature-dependent magnetization (M - T) of Cu_2OSeO_3 (Fig. 1) shows a cusp, which is seen in other skyrmion host B20 materials such as MnSi [30], FeGe [13,31], and $\text{Fe}_{0.8}\text{Co}_{0.2}\text{Si}$ [32]. The cusp in the M - T is emerging mainly due to the competition between SEI and antisymmetric DMI. The total magnetic moment can be expressed as, $M_{\text{expt}} = M_{\text{SEI}} + M_{\text{DMI}}$, where M_{expt} is the experimentally observed magnetic moment, M_{SEI} is the moment due to SEI, and M_{DMI} is the moment due to DMI. M_{SEI} has been extrapolated using the relation $M_{\text{SEI}} \propto (T_C - T)^\beta$, where β is the magnetization exponent. The peak position (or maximum) and minimum of dM/dT have been found to be at $T'_C = 58.22$ K and $T_C = 59.42$ K. The λ -like variation in the specific heat [17] and discontinuous change in magnetic entropy [16] identify the FOPT around T'_C . Shoulderlike variation in the specific heat, continuous variation in the change in entropy, and positive slope of M^2 versus $\mu_0 H/M$, known as the Arrott plot [33], confirm SOPT at T_C [16,17]. As discussed before, the DMI weakens faster compared to SEI after T'_C and this is responsible for the increase in the magnetization which can be explained as follows: in the helical phase, spins form helix with a pitch over which net magnetization is zero. In the skyrmionic phase, the spins form a helix on the diametric points of skyrmion with a pitch equal to the diameter of skyrmion. Again net magnetization for skyrmion is zero. The nonmonotonic temperature dependence of magnetization near T'_C and T_C can be explained as follows: (i) as temperature increases, DMI decreases substantially resulting breakage of spin textures which causes enhancement of magnetic moment, and (ii) further increase in temperature leads to evolution of FD phase, which causes lowering of magnetic moment.

Some groups have investigated the critical behavior of skyrmion host B20 materials by erroneously choosing maximum of the M - T as the transition temperature [31,34]. Generally, the critical behavior of a magnetic system should be studied around the transition temperature determined by the minimum of dM/dT [13,30,32], above which order parameter becomes zero. Moreover, the actual T_C can be justified by the point of inflection in the specific heat, magnetization, and susceptibility, and the maximum of change in entropy at T_C . To investigate the critical behavior in Cu_2OSeO_3 , we have used the Arrott-Noakes relation [35], which is given by $(\mu_0 H/M)^{1/\gamma} = (T - T_C)/T_C + (M/M_1)^{1/\beta}$, where M_1 is a temperature and field-dependent constant. $(\mu_0 H/M)^{1/\gamma}$ versus $M^{1/\beta}$ plots, which are known as modified Arrott plots (MAPs), were obtained using the β and γ values of the standard 3D models. By fitting with linear curves in the high field region of the MAPs, normalized slopes (NSs) were estimated [13] as shown in Fig. 2(a). NS is defined as $\text{NS} = S(T)/S(T_C)$, where $S(T)$ is the slope of the linear fit to the MAPs at temperature T and $S(T_C)$ is the slope of the linear fit to the MAP at temperature T_C . The critical behavior of a

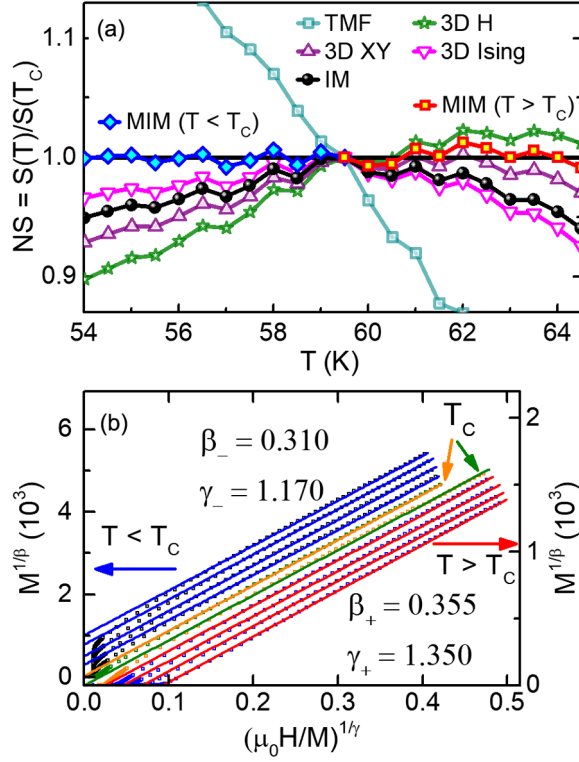


FIG. 2. (a) Normalized slope, $NS = S(T)/S(T_C)$, plots constructed using the critical exponents of standard 3D models, obtained by iteration method, and estimated from the modified iteration method (MIM) for $T < T_C$ and $T > T_C$. (b) MAPs of Cu_2OSeO_3 constructed using the critical exponents obtained from MIM. H , Heisenberg; IM, iteration method. TMF, tricritical mean-field.

magnetic material will follow a single UC if the NSs obtained from the critical exponents lead to a constant slope, i.e., 1 or close to 1, irrespective of the temperature being below or above T_C . In contrast to standard and trivial magnetic systems, this primary inspection leads to the crossover in the critical behavior of Cu_2OSeO_3 from 3D Ising (below T_C) to 3D Heisenberg UC (above T_C).

Iteration method is most frequently used to determine the critical exponents [36]. Figure 2(a) shows the results from the iteration method, which yields $\beta = 0.343 \pm 0.010$ and $\gamma = 1.206 \pm 0.020$ [20]. It is clear that the deviation is unusually large in the temperature dependence of the NS plot. The large deviation in the NS plot indicates that iteration method is inapplicable in Cu_2OSeO_3 for the reasons discussed above. The issue in the iteration method is that field-dependent magnetization (M - H) isotherms are fitted with the same set of critical exponents below and above T_C . This leads to identical critical behavior below and above T_C . To address this problem, we have proposed a new method, MIM, to analyze the critical behavior of Cu_2OSeO_3 —a nontrivial system. In our MIM, we divided the M - H isotherms in two sets—one for $T \leq T_C$ and the other one for $T \geq T_C$.

The MIM to determine the critical exponents is as follows. (i) Take two sets of M - H isotherms, the first one for $T \leq T_C$ and the second one for $T \geq T_C$. It means M - H taken at T_C will be common in both sets. Now, select one set of M - H isotherms for analysis. (ii) Take the critical exponents (β and γ) of that particular UC, which show NSs [see Fig. 2(a)] close to 1. (iii) Vary β and γ in such a way that the NSs obtained from the constructed MAPs approach closer to 1. In the whole process, vary β and γ maintaining T_C unaltered. (iv) When NSs converge to 1, stop the process. Thus, the critical exponents, β_- and γ_- for $T \leq T_C$ or β_+ and γ_+ for $T \geq T_C$, will be determined. Otherwise, repeat steps (ii) and (iii) till NSs converge to 1. Repeat the above processes by selecting the remaining other set of the M - H isotherms. Thus, $(\beta_- : \gamma_-) = (0.310 \pm 0.010 : 1.170 \pm 0.005)$ for $T < T_C$ and $(\beta_+ : \gamma_+) = (0.355 \pm 0.005 : 1.350 \pm 0.005)$ for $T > T_C$ have been obtained [Fig. 2(a)]. The self-consistency and reliability of these critical exponents were checked by Widom scaling relation ($\delta = \gamma/\beta + 1$), which gives δ values ($\delta_- = 4.77 \pm 0.16$ below T_C and $\delta_+ = 4.80 \pm 0.09$ above T_C) close to the value of $\delta = 4.63 \pm 0.01$ obtained from the M - H taken at T_C using $M = D(\mu_0 H)^{1/\delta}$, where D is a constant. The MAPs obtained from the MIM are shown in Fig. 2(b) [20].

It is required to estimate the range and spin dimensionality (n) in Cu_2OSeO_3 to confirm the appropriate UC with the help of critical exponents determined by the MIM. According to RG theory [28,29], the range of magnetic interaction depends on the exchange distance $J(r)$ [37], which decays with distance r as $J(r) \approx r^{-(d+\sigma)}$, where d and σ are the spatial dimensionality and constant, respectively. $\sigma \leq 3/2$ satisfies the mean-field model ($\beta = 0.5$, $\gamma = 1$) and $\sigma \geq 3/2$ implies short-range magnetic interaction. The relation of γ with d , n and σ is $\gamma = 1 + (4/d) [(n+2)/(n+8)]\Delta\sigma + \{[8(n+2)(n-4)]/[d^2(n+8)^2]\} \{1 + [2G(d/2)(7n+20)]/[(n-4)(n+8)]\}\Delta\sigma^2$, where $\Delta\sigma = [\sigma - (d/2)]$ and $G(d/2) = 3 - (1/4)(d/2)^2$. Those values of d , n , and σ will be valid if the values of β , γ , and δ are close to their experimental values [19,38,39]. The critical exponents obtained from the MIM yield $(d:n:\sigma) = (3:1:1.80 \pm 0.01)$ below T_C and $(d:n:\sigma) = (3:3:1.91 \pm 0.008)$ above T_C . This implies that $J(r)$ varies as $\sim r^{-4.80}$ and $\sim r^{-4.91}$ below and above T_C , respectively. Hence, the critical behavior of Cu_2OSeO_3 is 3D Ising ($n = 1$) type below T_C and 3D Heisenberg ($n = 3$) type above T_C . The essence of MIM is as follows: same values of n will yield identical critical behavior below and above T_C —a *trivial situation*, and different values of n will yield different critical behavior below and above T_C —a *nontrivial situation*. Thus, it can be concluded that MIM is a general method for critical analysis and iteration method is a special case of MIM. It can be argued that magnetocrystalline anisotropy and anisotropy due to spin-orbit coupling, which actually gives rise to DMI in these systems, are responsible for 3D Ising-type interaction below T_C . It will

be interesting to show theoretically how the presence of DMI and different anisotropic interactions with SEI give rise to effective anisotropic exchange interaction responsible for various topological spin textures below T_C . Using RG theory and exact numerical diagonalization methods [40], it has been shown that twisting in the spins may be observed in Ising systems in the presence of DMI.

The scaling equation of a magnetic system is given as $M(H, \epsilon) = e^\beta f_\pm(H/\epsilon^{\beta+\gamma})$, where f_\pm are regular functions such as f_+ for $T > T_C$ and f_- for $T < T_C$ [19,27,41]. Let us define the renormalized magnetization as $m = M|\epsilon|^{-\beta}$ and renormalized field as $h = \mu_0 H |\epsilon|^{-(\beta+\gamma)}$. Two universal curves (m versus h) were obtained below and above T_C [Fig. 3(a)] using the critical exponents $\beta_- = 0.310 \pm 0.010$, $\gamma_- = 0.170 \pm 0.005$ for $T < T_C$ and $\beta_+ = 0.355 \pm 0.005$,

$\gamma_+ = 1.350 \pm 0.005$ for $T > T_C$ [20]. For further corroboration, the renormalized Arrott-plots (RAPs), i.e., m^2 versus h/m [42], has been plotted and shown in Fig. 3(b). Two separate universal curves have been obtained in RAPs. Thus, scaling results justify the method proposed here. The log-log plot of both scaled [inset of Fig. 3(a)] and RAPs [inset of Fig. 3(b)] show deviation from the universal curve in low field. This deviation can be understood as follows: if there were only 3D Ising exchange interaction below T_C , then all the isothermal curves would have collapsed onto the universal curve. However, the deviation from universal curve in the low field indicates the presence of another interaction in addition to the Ising interaction and that is DMI, which cannot exist at high field. This can be accounted from the Hamiltonian for DMI, $\mathcal{H}_{\text{DMI}} = -\sum_{ij} \vec{D}_{ij} \cdot (\vec{S}_i \times \vec{S}_j)$, where \vec{S}_i and \vec{S}_j are the spins at the i th and j th site, respectively. As the field increases, \mathcal{H}_{DMI} vanishes and this causes universal scaling at high field. Figure 3(c) shows the M - H taken at 5 K. After ≈ 150 mT, the saturation magnetization becomes $0.53\mu_B/\text{Cu}^{2+}$, which is due to 3(up):1(down) spin configuration. So, the spins are aligned parallel (or antiparallel) to each other in the high field region (≥ 150 mT). This, further, elaborates the excellent scaling in the high field region but not in the low field region due to presence of DMI.

The expanded view of the log-log plot of the RAPs [Fig. 3(d)] show multiple positive and negative slopes in low field. The phase boundaries constructed from the multiple slopes match well with the reported phase diagrams [4,11,15,16]. Thus, it can be argued that the first positive slope in the RAPs represent the MDH phase. The next negative slope is due to the SDC phase. A positive slope appears in the SDC phase from ~ 55 to ~ 58 K, and the field range from ~ 8 to ~ 21 mT. This region belongs to the skyrmion phase. After SDC, positive slope appears in high field. The noticeable point is that the multiple phases are below 58.5 K because the curve at 58.5 K shows only positive slope in the whole field region. No negative slope in the curve at 58.5 K implies that the helimagnetic phase transition line is below 58.5 K. It also implies the existence of weak DMI above T'_C (Fig. 1) corroborating the existence of the FD phase [16,29] between T'_C and T_C . Based on RAPs analyses, the phase boundaries of MDH to SDC, SDC to skyrmion, and SDC to field polarized (H_C) phase can be estimated. With the help of our entropic [16] and M - T analyses [20], we have estimated the phase boundaries connecting the FD phase and paramagnetic phase. Figure 3(e) shows the constructed phase diagram using the above analyses. To determine the order of phase transition between different phases, specific heat [1,17], change in entropy [16], and Banerjee's criteria [43] have been employed. The tricritical point and the Lifshitz point have been found at $\sim (57.5 \text{ K}, 31 \text{ mT})$ and $\sim (58.8 \text{ K}, 30 \text{ mT})$, respectively. As shown in Fig. 3(e), skyrmionic, SDC, and FD phases are meeting at two

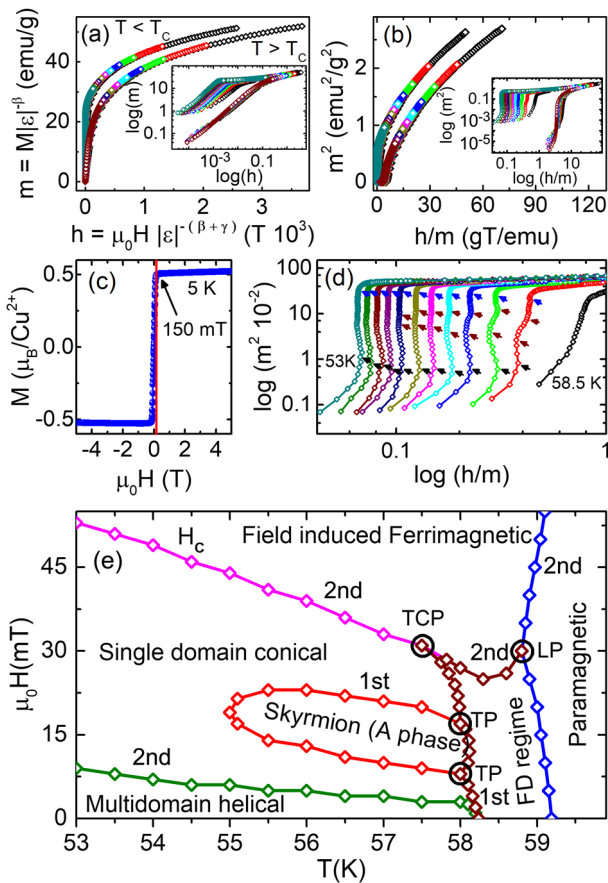


FIG. 3. (a) Scaled data of Cu_2OSeO_3 using scaling equation of state. Two universal curves are observed below and above T_C . Inset: log-log plot of the scaled data. (b) Renormalized Arrott-plots (RAPs) of the scaled data of Cu_2OSeO_3 . Inset: log-log plot of the RAPs. (c) M - H curve taken at 5 K. Saturation magnetization of $\approx 0.53\mu_B/\text{Cu}^{2+}$ ion reveals ferrimagnetic ordering above 150 mT. (d) Expanded view of the log-log plot of the RAPs below T_C . Arrows represent the schematic phase boundary points. (e) Phase diagram constructed using the RAPs of Cu_2OSeO_3 , M - T taken at various fields, and previous reports [7,16,17,43]. TCP, tricritical mean-field; TP, triple point; LP, Lifshitz point.

different points at $\sim(58 \text{ K}, 8 \text{ mT})$ and $\sim(58 \text{ K}, 17 \text{ mT})$ on the FOPT boundary line. This indicates that these two points should be the triple point in Cu_2OSeO_3 as shown in Fig. 3(e).

In conclusion, critical analysis of magnetization in Cu_2OSeO_3 shows the existence of different critical exponents below and above the transition point. This nontrivial situation can be dealt with the proposed method that can be applied to any systems, having SOPT, in which the nature of interactions is different on two sides of the transition. In fact, the proposed method is applicable both in trivial as well as in nontrivial systems. We have further shown that the phase diagram of Cu_2OSeO_3 can be obtained from this critical analysis. The constructed phase diagram shows the existence of tricritical point, Lifshitz point, and triple point in Cu_2OSeO_3 . A combined theoretical and experimental investigation is required to reveal the microscopic origin behind the different UCs of critical behavior for $T < T_C$ and $T > T_C$.

We thank AIRF-JNU for providing facilities for PPMS and XRD measurement. H. C. C. acknowledges UGC-CSIR for financial support through a fellowship.

*subhasis.ghosh.jnu@gmail.com

- [1] S. Mühlbauer, B. Binz, F. Jonietz, C. Pfleiderer, A. Rosch, A. Neubauer, R. Georgii, and P. Böni, *Science* **323**, 915 (2009).
- [2] H. Wilhelm, M. Baenitz, M. Schmidt, U. K. Rößler, A. A. Leonov, and A. N. Bogdanov, *Phys. Rev. Lett.* **107**, 127203 (2011).
- [3] W. Münzer, A. Neubauer, T. Adams, S. Mühlbauer, C. Franz, F. Jonietz, R. Georgii, P. Böni, B. Pedersen, M. Schmidt, A. Rosch, and C. Pfleiderer, *Phys. Rev. B* **81**, 041203(R) (2010).
- [4] S. Seki, X. Z. Yu, S. Ishiwata, and Y. Tokura, *Science* **336**, 198 (2012).
- [5] T. Lancaster, R. C. Williams, I. O. Thomas, F. Xiao, F. L. Pratt, S. J. Blundell, J. C. Loudon, T. Hesjedal, S. J. Clark, P. D. Hatton, M. Ciomaga Hatnean, D. S. Keeble, and G. Balakrishnan, *Phys. Rev. B* **91**, 224408 (2015).
- [6] X. Yu, Y. Tokunaga, Y. Taguchi, and Y. Tokura, *Adv. Mater.* **29**, 1603958 (2017).
- [7] A. Bauer, M. Garst, and C. Pfleiderer, *Phys. Rev. Lett.* **110**, 177207 (2013).
- [8] I. Dzyaloshinsky, *J. Phys. Chem. Solids* **4**, 241 (1958).
- [9] T. Moriya, *Phys. Rev.* **120**, 91 (1960).
- [10] D. Kim, B. L. Zink, F. Hellman, and J. M. D. Coey, *Phys. Rev. B* **65**, 214424 (2002).
- [11] D. R. Nelson, *Phys. Rev. B* **13**, 2222 (1976).
- [12] F. Léonard and B. Delamotte, *Phys. Rev. Lett.* **115**, 200601 (2015).
- [13] L. Zhang, H. Han, M. Ge, H. Du, C. Jin, W. Wei, J. Fan, C. Zhang, L. Pi, and Y. Zhang, *Sci. Rep.* **6**, 22397 (2016).
- [14] H. Omrani, M. Mansouri, W. Cheikhrouhou Koubaa, M. Koubaaa, and A. Cheikhrouhoua, *RSC Adv.* **6**, 78017 (2016).
- [15] S. Seki, J. H. Kim, D. S. Inosov, R. Georgii, B. Keimer, S. Ishiwata, and Y. Tokura, *Phys. Rev. B* **85**, 220406(R) (2012).
- [16] H. C. Chauhan, B. Kumar, J. K. Tiwari, and S. Ghosh, *Phys. Rev. B* **100**, 165143 (2019).
- [17] T. Adams, A. Chacon, M. Wagner, A. Bauer, G. Brandl, B. Pedersen, H. Berger, P. Lemmens, and C. Pfleiderer, *Phys. Rev. Lett.* **108**, 237204 (2012).
- [18] M. Janoschek, M. Garst, A. Bauer, P. Krautscheid, R. Georgii, P. Böni, and C. Pfleiderer, *Phys. Rev. B* **87**, 134407 (2013).
- [19] F. Qian, L. J. Bannenberg, H. Wilhelm, G. Chaboussant, L. M. Debeer-Schmitt, M. P. Schmidt, A. Aqeel, T. T. M. Palstra, E. Brück, A. J. E. Lefering, C. Pappas, M. Mostovoy, and A. O. Leonov, *Sci. Adv.* **4**, eaat7323 (2018).
- [20] See Supplemental Material at <http://link.aps.org/supplemental/10.1103/PhysRevLett.128.015703>, which also includes Refs. [21–23], for details on crystal structure, experimental details, specific heat, Arrott plot, modified Arrott plot, iteration method, determination of critical exponents from entropy analysis, scaling results, estimation of field-dependent T'_C and T_C , and table of critical exponents of standard 3D models and Cu_2OSeO_3 estimated using various methods.
- [21] B. H. Toby, *Powder Diffr.* **21**, 67 (2006).
- [22] H. Irfan, K. Mohamed Racik, and S. Anand, *J. Asian Ceram. Soc.* **6**, 54 (2018).
- [23] M. E. Fisher, *Rep. Prog. Phys.* **30**, 615 (1967).
- [24] J. S. White, I. Levatić, A. A. Omrani, N. Egetenmeyer, K. Prša, I. Živković, J. L. Gavilano, J. Kohlbrecher, M. Bartkowiak, H. Berger, and H. M. Rønnow, *J. Phys. Condens. Matter* **24**, 432201 (2012).
- [25] J. H. Yang, Z. L. Li, X. Z. Lu, M.-H. Whangbo, and Su—Huai Wei, X. G. Gong, and H. J. Xiang, *Phys. Rev. Lett.* **109**, 107203 (2012).
- [26] S. Schlotter, P. Agrawal, and G. S. D. Beach, *Appl. Phys. Lett.* **113**, 092402 (2018).
- [27] Y. Zhou, R. Mansell, S. Valencia, F. Kronast, and S. van Dijken, *Phys. Rev. B* **101**, 054433 (2020).
- [28] K. G. Wilson, *Rev. Mod. Phys.* **55**, 583 (1983).
- [29] M. E. Fisher, *Rev. Mod. Phys.* **46**, 597 (1974).
- [30] L. Zhang, D. Menzel, C. Jin, H. Du, M. Ge, C. Zhang, L. Pi, M. Tian, and Y. Zhang, *Phys. Rev. B* **91**, 024403 (2015).
- [31] H. Wilhelm, A. O. Leonov, U. K. Rössler, P. Burger, F. Hardy, C. Meingast, M. E. Gruner, W. Schnelle, M. Schmidt, and M. Baenitz, *Phys. Rev. B* **94**, 144424 (2016).
- [32] W. Jiang, X. Z. Zhou, and G. Williams, *Phys. Rev. B* **82**, 144424 (2010).
- [33] A. Arrott, *Phys. Rev.* **108**, 1394 (1957).
- [34] I. Živković, J. S. White, H. M. Rønnow, K. Prša, and H. Berger, *Phys. Rev. B* **89**, 060401(R) (2014).
- [35] A. Arrott and J. Noakes, *Phys. Rev. Lett.* **19**, 786 (1967).
- [36] J. K. Tiwari, H. C. Chauhan, B. Kumar, and S. Ghosh, *J. Phys. Condens. Matter* **32**, 195803 (2020).

- [37] V. Franco, J. S. Blázquez, and A. Conde, *Appl. Phys. Lett.* **89**, 222512 (2006).
- [38] M. E. Fisher, Shang-keng Ma, and B. G. Nickel, *Phys. Rev. Lett.* **29**, 917 (1972).
- [39] L. Zhang, D. Menzel, H. Han, C. Jin, H. Du, J. Fan, M. Ge, L. Ling, C. Zhang, L. Pi, and Y. Zhang, *Europhys. Lett.* **115**, 67006 (2016).
- [40] R. Jafari, M. Kargarian, A. Langari, and M. Siahatgar, *Phys. Rev. B* **78**, 214414 (2008).
- [41] H. E. Stanley, *Rev. Mod. Phys.* **71**, S358 (1999).
- [42] S. Kaul, *J. Magn. Magn. Mater.* **53**, 5 (1985).
- [43] S. K. Banerjee, *Phys. Lett.* **12**, 16 (1964).